Sensors & Transducers, Vol. 203, Issue 8, August 2016, pp. 24-32

Sensors & Transducers

http://www.sensorsportal.com

Filling of Parallel Microchannel Networks: Analysis of the De-synchronization

[1, *] Jean BERTHIER, [1] Guillaume DELAPIERRE, [2] M. Lemine DIAKITE and [1] Fabrice NAVARRO

[1] Univ. Grenoble Alpes F-38000 Grenoble, France

[1] CEA, LETI, MINATEC Campus, F-38054, Grenoble, France

[2] Fondation Méditerranée Infection, Unité de Recherche sur les Maladies Infectieuses et Tropicales Émergentes (URMITE) UMR 6236 Faculté de médecine 27 Bd Jean Moulin, F-13385 Marseille Cedex 05, France

[*] E-mail: jean.berthier@cea.fr

Received: 29 July 2016 /Accepted: 28 August 2016 /Published: 31 August 2016

Abstract: Point-of-care (POC) reaction microchambers are basis features of biotechnological devices. Most of the time biotechnological devices comprise multiple reaction chambers, in order to achieve simultaneously as many reactions as possible, enhancing the efficiency of these devices. Parallelization requires the precise filling and loading of these chambers, and the best synchronization is searched for. De-synchronization triggers the formation of air bubbles and leads to anomalous functioning of the device.

It has been observed that synchronized filling of microchannels and fluidic networks is often an experimental challenge. In fact, this experimental difficulty directly stems from the conceptual approach of the design of the network.

In this work we theoretically investigate the filling of networks, driven by the injection pressure of a pump. The additional effect of capillary forces is also taken into account. Experimental results are compared with the theoretical model. Rules for better synchronization are enounced. *Copyright © 2016 IFSA Publishing, S. L.*

Keywords: Network, Parallel chambers, Synchronization, Pump pressure, Pressure drop, Capillary pressure, Laplace pressure.

1. Introduction

Reaction microchambers are basis features of many biotechnological devices. Most of the time biotechnological devices comprise multiple reaction chambers, in order to achieve simultaneously as many reactions as possible in order to enhance the potentialities of the device and the speed of analysis. The examples are many in the literature. They go from DNA sequencing – where massively parallel DNA sequencing is revolutionizing genomics research [1], to gene amplification by polymerase chain reactions (PCR) [2], to cell culture [3], and to biochemical reactions [4].

These chambers are usually connected to an input port and an output port by a fluidic network. Parallelization requires the precise filling and loading of these chambers, and the best synchronization is searched for. De-synchronization triggers the formation of air bubbles and leads to anomalous functioning of the device. In the case of PCR amplification, trapped bubbles will expand during the

thermal cycles, chasing the liquids, and preventing the amplification [5]. Air bubbles are also a considerable drawback for multi-wells cell culture [6]. Air bubbles trapping at the inlet of a network has been theoretically investigated by Bruus [7], but this analysis only concerns the network entrance and not the entity of the network.

An obvious solution to synchronize flows in networks is the use of valves controlling locally the filling of each of the channels of the network [8-9]. Such a solution requires the use of a large number of valves and complicates substantially the conception, fabrication, cost and use of these devices.

Hence an approach to reduce de-synchronization by passive means is of great interest. Indeed, it has been observed that the synchronized filling of microchannels – and more generally of fluidic networks – is often an experimental challenge. In fact, this experimental difficulty directly stems from the conceptual approach of the design of the network. A physical analysis of the causes of de-synchronization is then needed, taking into account that pump pressure and capillary pressure both contribute to the filling behavior.

Note the circulation of fluids in fully filled networks has been largely investigated, but our concern is the filling of the devices [10-12]. So far there has been few reports on the filling of networks in the literature. Kim and coworkers have investigated the capillary filling of parallel channels, Fig.1 [13].

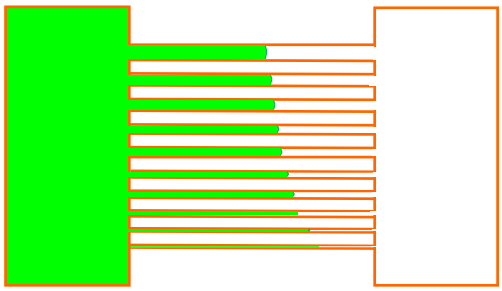

Fig. 1. Kim's analysis of the flow in parallel channels [13].

Numerical approach of the filling of a single micro-well under the conjugate effects of pump pressure and wall wettability has been reported by Tseng and colleagues [14], but a comprehensive approach of the synchronized filling of networks under the conjugate action of pump pressure and wettability forces is still missing.

In this work we first theoretically investigate the filling behavior of networks, using pump driven flows. The effect of capillary forces is later included in the model. Experimental results – obtained in a massively parallel RT-qPCR (real time quantitative polymerase chain reaction) chambers device [2] – are compared to the predictions of the theoretical model. Finally rules for better synchronization are enounced.

2. Theoretical Approach

Consider an initially empty microchannel, plugged to a pump. The pump forces liquid into the channel (Fig. 2). The liquid interface advances inside the channel with an average velocity noted *V*.

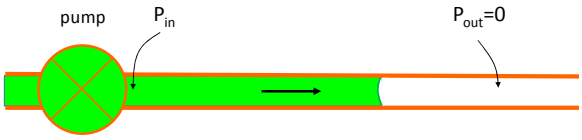

Fig. 2. Sketch of the channel.

Let us recall first that the pressure drop in a microchannel for a laminar flow is given by the general relation

$$\Delta P = R\,L\,Q\,, \tag{1}$$

where *P* is the pressure, *L* is the channel length, *R* is the hydraulic resistance *per unit length*, and *Q* is the volumic flow rate. Poiseuille and Hagen have first given an expression for the resistance *R* in the case of cylindrical tubes [15]; later, Shah and London have derived an expression for the hydraulic resistance for rectangular duct derived from a Fourier series expression [16]. There are now tables where the hydraulic resistances are listed for many different channel cross sections [7, 12, 17, 18].

Relation (1) assumes an established flow. Let us consider (1) differently, from a transient point of view, and base our reasoning by considering that the transient flow is always established approximately everywhere. This approximation is valid except at the very front of the advancing flow (Fig. 3).

Relation (1) can then be reinterpreted as

$$P_{in} = R\,z\,S\,\frac{dz}{dt}\,, \tag{2}$$

if we assume that the pressure at the front end is zero, i.e. if we neglect the capillary Laplace pressure.

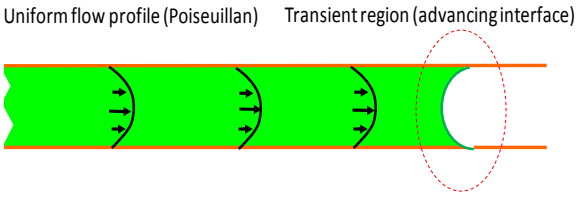

Fig. 3. Established region and front end of the flow.

In (2), *S* is the cross-sectional area of the channel and *z* the penetration length which is a function of the elapse time, and P_{in} is the inlet pressure.

Integration of (2) yields

$$z = \sqrt{\frac{2\,P_{in}}{R\,S}\,t} \tag{3}$$

The penetration distance varies as the square root of time. The time taken for filling the complete channel is then

$$\tau = \frac{L^2\,R\,S}{2\,P_{in}} \tag{4}$$

However, the role of capillarity has not been taken into account yet. In fact at the interface the Laplace pressure may play an important role depending on the wettability characteristics. The situation is sketched in Fig. 4.

We then rewrite (1) as

$$P_{in} - P_L = P_{in} - \gamma\kappa = R\,z\,S\,\frac{dz}{dt}, \tag{5}$$

where P_L is the capillary (Laplace) pressure, κ is the interface curvature and γ is the surface tension.

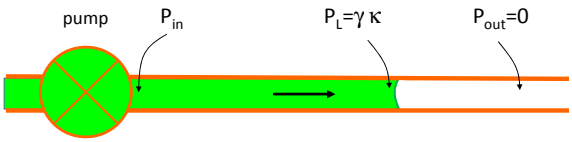

Fig. 4. Sketch of the channel, showing the interface contribution to the pressure field.

Introducing the wetted perimeter p, θ the contact angle, and D_H the hydraulic perimeter, relation (5) can be cast under the form

$$P_{in} + \frac{\gamma\,p\cos\theta}{S} = P_{in} + \frac{4\,\gamma\,\cos\theta}{D_H} = R\,z\,S\,\frac{dz}{dt} \tag{6}$$

Integration of (6) is straightforward, and we obtain

$$z = \sqrt{\frac{2\left(P_{in} + \dfrac{4\,\gamma\,\cos\theta}{D_H}\right)}{R\,S}\,t} \tag{7}$$

Note that if P_{in}=0, relation (7) reduces to the usual Lucas-Washburn-Rideal (LWR) expression [19-20] for the marching distance in a cylindrical tube. Denoting R_H the radius of the tube, the hydraulic resistance per unit length is

$$R = \frac{8\,\mu}{R_H^2}, \tag{8}$$

where μ is the dynamic viscosity of the liquid. Substituting in (7) yields the LWR law

$$z = \sqrt{\frac{\gamma\,\cos\theta\,r}{2\,\mu}\,t} \tag{9}$$

The real time taken for filling the complete channel of length L is then

$$\tau = \frac{L^2\,R\,S}{2\left(P_{in} + \dfrac{4\,\gamma\,\cos\theta}{D_H}\right)} \tag{10}$$

One can compare the two characteristic times – that including the Laplace pressure τ_L and that without the Laplace pressure τ_0 – to estimate the importance of the capillary contribution. Let us note the non-dimensional coefficient

$$\tilde{q} = \frac{P_{in}}{\dfrac{4\,\gamma\,\cos\theta}{D_H}}, \tag{11}$$

then the relative time error that is done when neglecting the capillary effect is

$$\frac{\Delta\tau}{\tau_0} = \frac{\tau_L - \tau_0}{\tau_0} = \frac{-sign(\tilde{q})}{\tilde{R} + 1} \tag{12}$$

In the case where $abs(\tilde{q}) >> 1$, the pressure from the pump dominates, and the time shift is negligible. However if $abs(\tilde{q}) < 1$ the capillary effect becomes important, and when $abs(\tilde{q}) << 1$ the time shift can be approximated by

$$\frac{\Delta\tau}{\tau_0} = \frac{\tau_L - \tau_0}{\tau_0} = -sign(\tilde{q}) \tag{13}$$

In the case of a lyophilic channel – the liquid wets the wall – the contact angle θ is less than 90°, and the coefficient $\tilde{q}$ is positive. Relation (12) indicates that the liquid arrives earlier than the expected time based on the pump pressure only. Conversely, the liquid progresses slower than expected in the case of a lyophobic contact angle. If the injection pressure P_{in} is small and the capillary force opposes the flow ($abs(\tilde{q}) << 1$ and $\theta > 90°$) the filling might even not take place. Fig. 5 illustrates the time required for filling a 10 cm long channel of 100 µm radius with water, depending on the contact angle and the pump pressure. In the case of $\theta > 110°$, and $P_{in} < 1000$ Pa, it is impossible to fill the channel.

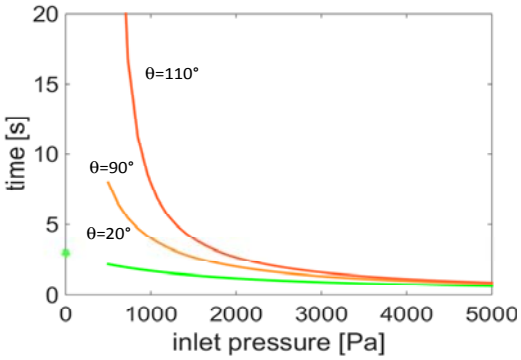

Fig. 5. Time required to fill the channel as a function of the pump pressure and the wall contact angle (L=10 cm, R=100 µm, μ=10^{-3} Pa.s, γ=72 mN/m).

3. Case of a Piecewise Constant Cross Section Channel

Relation (1) is valid for a constant cross-section channel. Now, consider a piecewise constant cross-section channel with n sections of length L_i, $i=1, n$ (Fig. 6). Without taking into account the capillary effect, relation (1) can be rewritten as

$$\Delta P = \left(\sum_i R_i \, L_i \right) Q \tag{14}$$

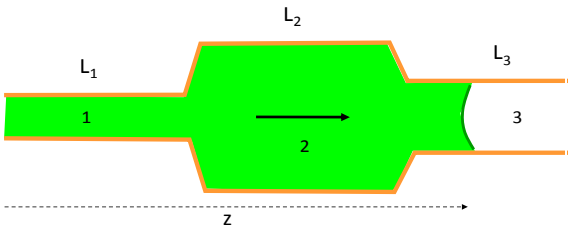

Fig. 6. Sketch of the channel with the different cross sections.

Using the same approach as before, with the liquid front in the n^{th} channel, as shown in Fig. 6, we obtain the relation

$$P_{in} = \left[\sum_{i=1}^{i=n-1} R_i \, L_i + R_n \left(z - \sum_{i=1}^{i=n-1} L_i \right) \right] S_n \frac{dz}{dt} \tag{15}$$

Integration of (15) yields

$$t - \sum_{i=1}^{i=n-1} \tau_i = \frac{S_n}{P_{in}} \left[\sum_{i=1}^{i=n-1} R_i \, L_i \left(z - \sum_{i=1}^{i=n-1} L_i \right) + \frac{R_n}{2} \left(z - \sum_{i=1}^{i=n-1} L_i \right)^2 \right], \tag{16}$$

where τ_i are the times for the flow to totally fill the channel i. The time lapse τ_n taken for the flow to totally fill the n^{th} channel is then

$$\tau_n = \frac{L_n \, S_n}{P_{in}} \left[\sum_{i=1}^{i=n-1} R_i \, L_i + \frac{R_n}{2} L_n \right] \tag{17}$$

This relation is valid for any index i. The flow front reaches the end of the n^{th} channel at the time

$$t_n = \sum_{i=1}^{i=n} \tau_i \tag{18}$$

We obtain an important result: Substitution of (17) – for each index i) – in (18) indicates that the time t_n is inversely proportional to P_{in}.

Note that, in order to take into account the capillary effect, the driving pump pressure P_{in} must be replaced by the total driving pressure (P_{in}+P_L), and the preceding relations must be rewritten as

$$\tau_n = \frac{L_n \, S_n}{\left(P_{in} + \dfrac{4 \gamma \cos\theta}{D_{Hn}} \right)} \left[\sum_{i=1}^{i=n-1} R_i \, L_i + \frac{R_n}{2} L_n \right], \tag{19}$$

where D_{Hn} is the hydraulic diameter of channel n. In the case of a pure capillary flow (P_{in}=0), it can be shown that relation (19) reduces to the generalized LWR law for piecewise constant cross section channels [21].

4. Synchronization of a Network

Parallel networks are ensembles of channels having a common inlet and a common outlet and a diversity of different channels and micro-chambers in parallel. An element of a network is sketched in Fig. 7.

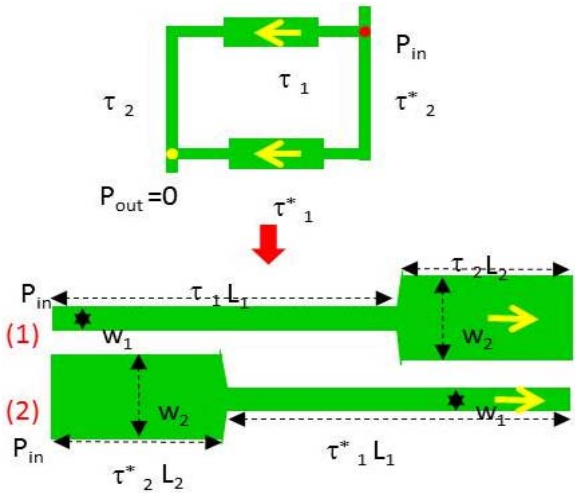

Fig. 7. Top: Schematic of a simple network, with two branches, and non-uniform cross sections; bottom: schematic of the two branches of the network (1) and (2), which are geometrically identical but in reverse direction for the flow.

We first schematize such an element by the two channels shown at the bottom of Fig. 6. We shall show next that, although these two channels comprise the same segments (in reverse order), they are not equivalent from a hydraulic point of view. Their filling process requires different time intervals.

Hence in the geometry of Fig. 7, synchronization is never achieved.

First, for simplicity of the reasoning, we only consider the pump pressure and neglect the capillary effects. We shall introduce later the corrections for the capillary effects.

The filling times for the two "symmetrical" channels shown in Fig. 7 are derived using the results of the preceding section.

According to (17), the time required for the flow to reach the extremity of first system is

$$t_{1,2} = \frac{L_1 S_1}{P_{in}}\left[\frac{R_1}{2}L_1\right] + \frac{L_2 S_2}{P_{in}}\left[R_1 L_1 + \frac{R_2}{2}L_2\right] \quad (20)$$

On the other hand, still according to (17), in the second system

$$t_{2,1} = \frac{L_2 S_2}{P_{in}}\left[\frac{R_2}{2}L_2\right] + \frac{L_1 S_1}{P_{in}}\left[R_2 L_2 + \frac{R_1}{2}L_1\right] \quad (21)$$

The two different geometries are not commutative: the time required to reach the channel outlet depends on the history of the flow in all the sections. The de-synchronization time is

$$\Delta t_{1,2} = t_{1,2} - t_{2,1} = \frac{L_1 L_2}{P_{in}}\left[S_2 R_1 - S_1 R_2\right] \quad (22)$$

De-synchronization is inversely proportional to P_{in} and proportional to the segment lengths L_1 and L_2, and to the contrast of cross section between segments 1 and 2 corresponding to the term S_2R_1-S_1R_2.

Expression (22) does not take into account the effect of capillarity. Using relation (19) where the capillary pressure has been introduced, instead of (17), the de-synchronization time can be written

$$\Delta t_{1,2} = t_{1,2} - t_{2,1} = \frac{L_1 L_2}{P_{in}}\left[\frac{S_2 R_1}{1+\frac{1}{\tilde{q}_2}} - \frac{S_1 R_2}{1+\frac{1}{\tilde{q}_1}}\right], \quad (23)$$

where $\tilde{q}_i = P_{in} \Big/ \frac{4\gamma\cos\theta}{D_{H_1}}$, for i=1, 2. The structure of relation (23) is similar to that of relation (22): neglecting the capillary effect brings back to relation (22). On the other hand, neglecting the pressure P_{in} compared to the capillary force yields.

Inspection of relations (22) and (23) shows that increasing the contrast between the two sections dimensions leads to an increase of the de-synchronization of the flows.

5. Generalization to PCR Parallel Networks

Real networks are more complicated than that considered in the preceding section. Consider the network shown in Fig. 8. Such a network is designed for the simultaneous PCR (polymerase chain reaction) amplification of DNA strands [2]. More specifically the network aims at the RT-qPCR, which stands for real-time quantitative PCR [22-23], for the detection of mutated genes.

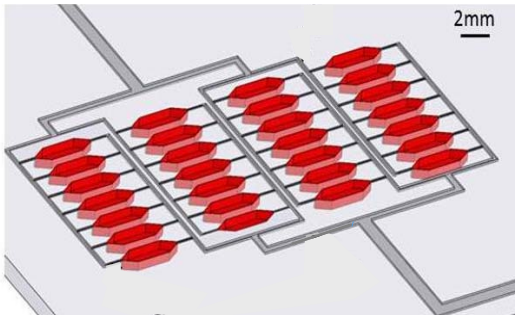

Fig. 8. View of the massively parallel device.

The network comprises 4×7 chambers feed with liquid sample in parallel (the reaction primers have been initially spotted in the chambers). A detailed view of an element of the network is shown in Fig. 9.

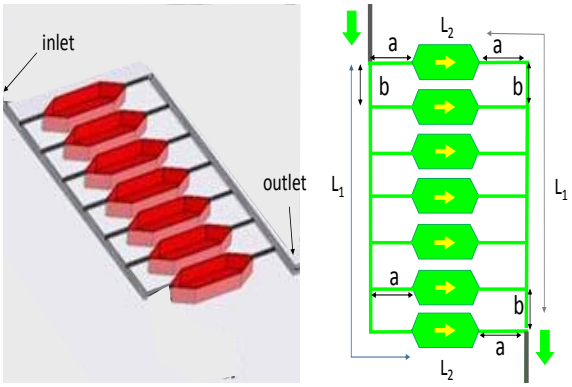

Fig. 9. Details of one element of the PCR device comprising 7 PCR chambers: left, perspective view of the 7 PCR chambers; right: sketch of the different rows of an element.

Although the situation is much more complicated than that studied in the preceding section, an approach can be done by considering the schematic of Fig. 10. Consider the top row and a row below corresponding to an index n (here n={1, .., 7}). We can consider three segments for each row (each branch of the network). The top row has the characteristics L_1=a, L_3=a+nb, while the bottom row has the opposite characteristics L_1=a+n b, L_3=a.

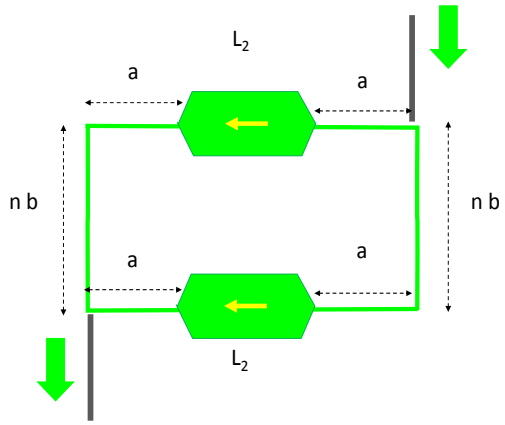

Fig. 10. Schematic of two branches of the PCR network. The distance *nb* corresponds to the n^{th} row in Fig. 9.

It is possible now to use relation (17) or (19) to calculate the time required for the flow to filling each channel. If capillary effects are neglected, one finds the de-synchronization time

$$\Delta t_{1,2} = \frac{1}{P_{in}}\left[L_1 L_2 \left(S_2 R_1 - S_1 R_2\right) + L_2 L_3 \left(S_3 R_2 - S_2 R_3\right)\right] \quad (24)$$

Under this form, relation (24) is just a generalization of (22).

The same approach can be done taking into account the capillary effect. One finds the formula

$$\Delta t_{1,2} = \frac{1}{P_{in}}\left[L_1 L_2 \left(\frac{S_2 R_1}{1+\frac{1}{\tilde{q}_2}} - \frac{S_1 R_2}{1+\frac{1}{\tilde{q}_1}}\right) + L_2 L_3 \left(\frac{S_3 R_2}{1+\frac{1}{\tilde{q}_3}} - \frac{S_2 R_3}{1+\frac{1}{\tilde{q}_2}}\right)\right] \quad (25)$$

Using the simplification that the channel cross section are identical outside of the chambers: $S_1=S_3$, $R_1=R_3$, (24) can be cast in the form

$$\Delta t_{1,2} = \frac{n b L_2}{P_{in}}\left(S_2 R_1 - S_1 R_2\right) \quad (26)$$

The de-synchronization time $\Delta t_{1,2}$ is negative showing that the flow in the top row is in advance compared to that in the other branches. The flow goes faster in the channel where the large section comes first. Relation (26) also shows that the de-synchronization is inversely proportional to P_{in}. On the other hand, it is proportional to n. Hence the de-synchronization with the first row increases from row to row. Finally it is proportional to L_2 (and indirectly to S_2): large reaction chambers inserted in the network increase the de-synchronization.

In the case of a non-negligible capillary effect, the same reasoning can be done starting from (25). One finds

$$\Delta t_{1,2} = \frac{n b L_2}{P_{in}}\left(\frac{S_2 R_1}{1+\frac{1}{\tilde{q}_2}} - \frac{S_1 R_2}{1+\frac{1}{\tilde{q}_1}}\right) \quad (27)$$

The same conclusions still hold. In the limit case of a purely capillary filling, relation (27) becomes

$$\Delta t_{1,2} = \frac{n b L_2}{4\gamma \cos\theta}\left(S_2 D_{H2} R_1 - S_1 D_{H1} R_2\right) \quad (28)$$

Again the flow in the top channel arrives first at the outlet, i.e. the capillary flow that passes first through the wide section arrives before that passing through the narrow section first. This property agrees with the results from [21, 24] developed otherwise.

6. Experimental Results and Discussion

The experimental device is a network designed for simultaneous PCRs for the amplification of ricin mutated DNA strands [2]. RT-qPCR (real time quantitative polymerase chain reaction) microchambers are disposed in a parallel disposition (Fig. 8 and Fig. 9).

PCR primers are first introduced in the microchambers. Then the device is sealed by a plastic cover. Finally the sample is introduced in the inlet port and penetrates the whole device under the action of a pump regulated in pressure (Fluigent ®, France). Different pump pressures have been tested for the filling of the device.

It is of utmost importance that no bubbles can form in the chambers. They would bias and even block the PCR reactions. In order to avoid the formation of bubbles, a synchronization of the incoming fluid must be achieved. De-synchronization produces trapped air bubbles in the device that migrates in the chambers and prevent the proper PCR processes.

The microfluidic network was drilled in PMMA (poly-methyl methacrylate), treated with plasma BSA (Bovine serum albumin), and covered with an optical pressure adhesive film (MicroAmp®, Lifes Technologies).

The walls have a contact angle with aqueous sample of approximately θ=60° and the cover film contact angle is θ_{top}=20°. The generalized Cassie angle derived in [25] – corresponding to the equivalent capillary force – is then given by the relation

$$\cos\theta^* = \frac{w}{2(w+h)}\cos\theta_{top} + \frac{w+2h}{2(w+h)}\cos\theta \quad (29)$$

Approximately θ^*=50°. The capillary term $\gamma cos\theta$ is then approximately 0.045 N/m, taking into account a surface tension γ=70 mN/m.

We decompose the problem in three cases: first, the pump pressure is large and dominates the capillary pressure; second the pump pressure is intermediate, but still dominates the capillary pressure; third, the pump pressure is small, and the effect of the capillary forces are important.

6.1. High Pump Pressures

First, the pump pressure is set to 1 Bar (10^5 Pa). The magnitude of the capillary pressure is approximately

$$P_{cap} \sim 2{,}8\frac{\gamma}{D_H} \sim \frac{0{,}2}{D_H} \tag{30}$$

Note that the Laplace pressure is negative because of the concavity of the interface. Numerically, P_{cap} ~ 1500 Pa for the smaller section channels, and only 50 in the microchambers.

In this case of high pump pressure, the capillary term at the denominator is negligible compared to the pressure P_{in} and relation (17) holds. The de-synchronization decreases as the inverse of the pump pressure: $\Delta t_{1,2} \sim \frac{1}{P_{in}}$; it is then expected that the de-synchronization delay should be small in this particular case.

We verify this behavior for the filling of the RT-qPCR microchambers device. This result can be seen in Fig. 11, where the system is synchronized. The different advancing interfaces in the chambers are delayed from a nearly constant time - pointed out by the dotted lines in the figure.

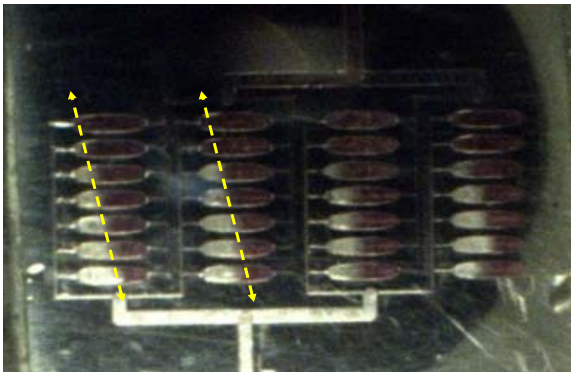

Fig. 11. Filling of the PCR device using high pump pressure (P_{in} = 1 Bar).

6.2. Moderate Pump Pressures

Let us set the injection pressure to 300 mBars (3×10^4 Pa). In this case, the capillary term is still negligible compared to the pressure term: the non-dimensional number representing the ratio between the pump pressure and the capillary pressure is larger than 30. The simplified relation (17) holds. However, due to the numerous branches of the fluidic network, some de-synchronization starts to appear (Fig. 12). The first rows of the device show synchronization – underlined by the dotted lines in the figure – but the bottom rows are somewhat de-synchronized. The theoretical analysis developed in the preceding section shows that the de-synchronization time is proportional to *nb*; hence it should be expected that the de-synchronization first appears in the bottom channels.

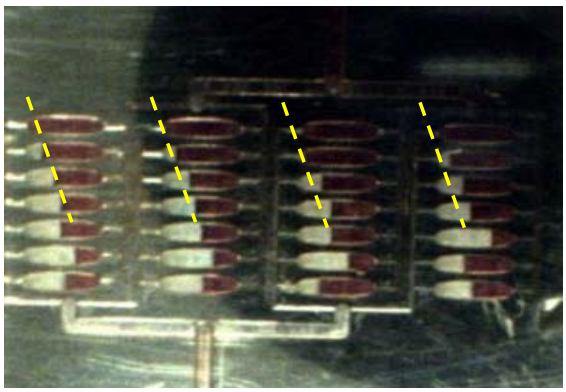

Fig. 12. Medium pump pressure (300 mBars): the first row only are synchronized.

6.3. Low Pump Pressures

In the case of low or very low inlet pressure (60 mBars or 6000 Pa), the capillary term cannot be neglected. The value of P_{cap} is small but not negligible compared to the inlet pressure P_{in}=6000 Pa in the small section channels. Conversely, the capillary effect is negligible in the large PCR chambers.

Fig. 13 shows the considerable de-synchronization in the bottom channels. The de-synchronization can be attributed at the same time to the pump pressure and capillary effects. In this case, we must refer to relation (19) because capillarity cannot be neglected.

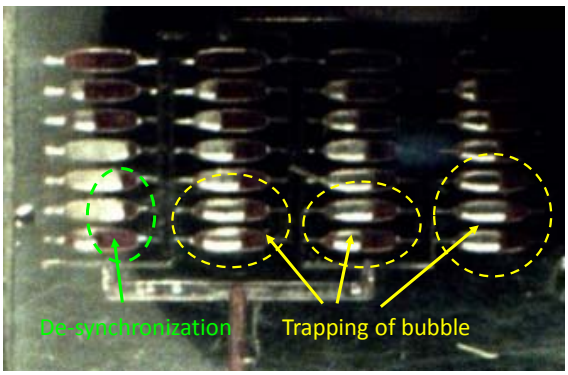

Fig. 13. Low pump pressure (60 mBars): desynchronization is visible in the bottom chambers, and bubbles are trapped.

7. Discussion and Conclusion

In this work, a theoretical analysis of the filling of a fluidic network has been performed. An expression for the travel time in the channels comprising different cross sectional areas has been derived and the de-synchronization time between two channels is determined. The model includes both the effects of the injection pump pressure and the capillary pressure. A non-dimensional number characterizing the relative importance of the capillary pressure is pointed out by the model.

It is shown that the de-synchronization time is inversely proportional to the injection pressure, and proportional to the dimensions of the microchambers, and to the connection lengths. In the case of low injection pressure, wettability effects considerably affect the synchronization.

In conclusion, synchronized filling of a fluidic network is difficult to achieve. This work shows that three solutions can improve the synchronization of the filling: first, applying a large injection pump pressure at the inlet is very advantageous. One has to be careful that the bonding of the cover plate should withstand such high pressure. In our case a maximum pressure of 1 bar does not constitute a real drawback. Second, the reduction of the size of the microchambers – in comparison with the connection channels hydraulic diameters – improves the synchronization of the filling of the network.

Finally, a numerical program for the optimization of the network can be set up using the transit time expressions in each subchannel.

References

[1]. J. Sandberg, Massively parallel analysis of cells and nucleic acids. Doctoral thesis in biotechnology, *KTH*, Stockholm, Sweden, 2011.

[2]. M. L. Diakite, J. Rollin, D. Jary, J. Berthier, C. Mouton-Gilles, D. Sauvaire, C. Philippe, G. Delapierre, X. Gidrol, Point-of-care diagnostics in ricin exposure, *Lab Chip*, Vol. 15, No. 10, 2015, pp. 2308-2317.

[3]. M. Mehling, S. Tay, Microfluidic cell culture, *Current Opinion in Biotechnology*, Vol. 25, 2014, pp. 95-102.

[4]. H. Kang Joo, Je-Kyun Park, ELISA reader compatible microfluidic device for enzyme kinetics, in *Proceedings of the Micro Total Analysis Systems*, Vol. 2, 2004, pp. 28-30.

[5]. R. S. Wiederkehr, B. Jones, S. Peeters, T. Stakenborg, O. Ibrahim, P. Fiorini, H. Tanaka, I. Yamashita, T. Matsuno, L. Lagae, On-chip multiplex PCR amplification directly from whole blood, in *Proceedings of the 17th International Conference on Miniaturized Systems for Chemistry and Life Sciences*, Freiburg, Germany, 27-31 October 2013, pp. 1776-1778.

[6]. L. Kim, Y.-C. Toh, J. Voldman, H. Yu, A practical guide to microfluidic perfusion culture of adherent mammalian cells, *Lab Chip*, Vol. 7, No. 6, 2007, pp. 681-694.

[7]. H. Bruus, Theoretical microfluidics, *Oxford University Press*, 2007.

[8]. M. A. Unger, H. P. Chou, T. Thorsen, A. Scherer, S. R. Quake, Monolithic microfabricated valves and pumps by multilayer soft lithography, *Science*, Vol. 288, Issue 5463, 2000, pp. 113-116.

[9]. A. K. Au, Hoyin Lai, B. R. Utela, A. Folch, Microvalves and micropumps for BioMEMS, *Micromachines*, Vol. 2, 2011, pp. 179-220.

[10]. I. Papautsky, J. Brazzle, T. Ameel, A. B. Frazier, Laminar fluid behavior in microchannels using micropolar fluid theory, *Sensors and Actuators A: Physical*, Vol. 73, 1999, pp. 101-108.

[11]. A. Ajdari, Steady flows in networks of microfluidic channels: building on the analogy with electrical circuits, *C. R. Physique*, Vol. 5, No. 5, 2004, pp. 539-546.

[12]. J. Berthier, P. Silberzan, Microsystems for biotechnology, 2nd edition, *Artech House Publishing*, 2012.

[13]. Dong Sung Kim, Kwang-Cheol Lee, Tai Hun Kwon, Seung S. Lee, Micro-channel filling flow considering surface tension effect, *Journal of Micromechanics and Microengineering*, Vol. 12, No. 3, 2002, pp. 236-246.

[14]. F.-G. Tseng, L.-D. Yang, K.-H. Lin, K.-T. Ma, M.-C. Lu, Y.-T. Tseng, C.-C. Chieng, Fluid filling into micro-fabricated reservoirs, *Sensors and Actuators A: Physical*, Vol. 97-98, 2002, pp. 131-138.

[15]. S. P. Sutera, The history of Poiseuille's law, *Ann. Rev. Fluid. Mech.*, Vol. 25, 1993, pp. 1-19.

[16]. R. K. Shah, A. L. London, Laminar flow forced convection in ducts, Advances in Heat Transfer Series, Supp. 1, *Academic Press*, New York, 1978.

[17]. K. V. Sharp, R. J. Adrian, J. G. Santiago, J. I. Molho, Liquid flows in microchannels, in MEMS: Introduction and fundamentals, editor M. Gad-El-Hak, *CRC Press*, Hoboken, 2005.

[18]. M. Bahrami, M. M. Yovanovich, J. R. A Culham, A novel solution for pressure drop in singly connected microchannels of arbitrary cross-section, *International Journal of Heat and Mass Transfer*, Vol. 50, 2007, pp. 2492-2502.

[19]. R. Lucas, Ueber das Zeitgesetz des Kapillaren Aufstiegs von Flussigkeiten, *Kolloid-Zeitschrift*, Vol. 23, No. 1, 1918, pp. 15-22.

[20]. E. W. Washburn, The dynamics of capillary flow, *Phys. Rev*., Vol. 17, 1921, pp. 273-283.

[21]. Berthier J., Gosselin D., Pham A., Delapierre G., Belgacem N., Chaussy D., Capillary flow resistors: local and global resistors, *Langmuir*, Vol. 32, No. 3, 2016, pp. 915-21.

[22]. S. A. Bustin, Absolute quantification of mRNA using real-time reverse transcription polymerase chain reaction assays, *J. Mol. Endocrinol*., Vol. 25, No. 2, 2000, pp. 169-193.

[23]. M. Kubista, J. M. Andrade, M. Bengtsson, A. Forootan, J. Jonák, K. Lind, R. Sindelka, R. Sjöback, B. Sjögreen, L. Strömbom, A. Ståhlberg, N. Zoric, The real-time polymerase chain reaction, *Molecular Aspects* of *Medicine*, Vol. 27, No. 2-3, 2006, pp. 95-125.

[24]. J. Berthier, D. Gosselin, A. Pham, F. Boizot, G. Delapierre, N. Belgacem, D. Chaussy, Spontaneous capillary flows in piecewise varying cross section microchannels, *Sensors and Actuators B: Chemical*, Vol. 223, 2016, pp. 868-877.

[25]. Berthier J., Brakke K., Berthier E., A general condition for spontaneous capillary flow in uniform cross-section microchannels, *Microfluid. Nanofluid. Journal*, Vol. 16, Issue 4, 2014, pp. 779-785.